Martian Unmanned Science Skimmer - Simulation

Draisey, S.[1] , Mullins, M.[1] , Samson C.[2] , Holladay, J.S.[3] , Lim D.[4]

[1] Good Vibrations Engineering Ltd., Nobleton, Ontario
sherry@gve.on.ca
[2] Dept. of Earth Sciences, Carleton University, Ottawa, Ontario
csamson@ccs.carleton.ca
[3] Geosensors Inc., 66 Mann Ave., Toronto, Ontario M4S 2Y3
scott.holladay@geosensors.com
[4] NASA Ames Research Center, Moffett Field, California
dlim@arc.nasa.gov

Abstract

This paper presents an early stage simulation of a specialized vehicle, targeted at providing controlled low altitude mobility over the Martian landscape, based on use of cold CO_2 propellant. The CO_2 propellant is extracted from the Martian atmosphere (95% CO_2, at 600 Pa).

The propulsion concept is based on the compression of atmospheric CO_2 overnight, for use as a cold propellant to hop in the morning. The vehicle is limited to Mars temperate or tropical zone landing sites, to utilize the temperature and pressure conditions which naturally support the CO_2 transition from gas to solid and back to gas. The power is provided by surface mounted solar cells.

The saucer-like planform of the vehicle is to provide maximize solar cell area, but also to maximize stance for landing gear. The consideration of rugged terrain and the destabilizing influence of ground effect aerodynamics on vehicle descent are yet to be established.

The simulation has been written to incorporate control parameters as the design matures. The simulation has allowed us to establish that differential thrust will provide sufficient vehicle control. The thrust response time is still assumed as instantaneous.

The vehicle science goals will be to use electro magnetic induction sounding to search for briny water/ice. The vehicle design is thus partially driven by minimizing moving metal components and vibration, to maximize the signal to noise ratio of the scientific instrument, the electromagnetic induction sounder (EMIS).

1.0 Introduction

The engineering design of our Martian science skimmer project is being driven through an in house software simulation. The simulation development is focussed on maximizing input from other engineering design packages, such as CAD drawings and finite element (FE) model outputs.

The design requirements are driven by a set of goals, developed for a proposed science mission, intended to search for near-surface briny water, in temperate and tropical regions of the Martian planet. The search for water is based on electromagnetic induction sounding (EMIS) mapping and a shallow drilling capability.

The simulations of the skimmer can be considered in two categories - hops intended for transportation and hops intended for subsurface geophysical mapping.

The engineering constraints of vehicle capability are driven by 3 factors; weight, electrical power and available propellant. Electrical power generation limits are based on solar cell area and sunlight intensity. The propellant considerations are driven by the Martian CO_2 density, available power and propellant gathering time.

We have chosen modest mobility goals, in the order of those being achieved by existing Martian rovers Spirit and Opportunity. Our maximum traverse goal is 15 meters per day.

The simulation development will be used to define control system parameters. In this paper, rotational control of the vehicle during hop has shown that directional control can be adequately achieved with differential throttling of three vertical thrusters. The rotational degrees of freedom were added to an existing simulation based solely on translation control. The translational control simulation was used to define the size of hops the vehicle would make. The simulation upgrade to rotational control is supported by FE modelling to predict pitch centre of gravity. The FE model has also been used to drive the design to ensure that the structure modes are above control frequency range.

2.0 Vehicle Configuration

The vehicle form, shown in Figure 1 is saucer shaped, with fixed tripod landing gear. The shape has been defined to maximize solar cell area. The main science instrument, 3 electromagnetic induction coils, are mounted within the shell of the structure, around 2 of the 6 CO_2 fuel tanks.

The structural components will be a composite material (fiberglas), to minimize electromagnetic noise on the science EMIS instrument. There will also be a shallow, subsurface drill, comprised of 3 drill rods - to allow maximum drill depth of 1 meter. The rods are positioned along the structure's vertical axis.

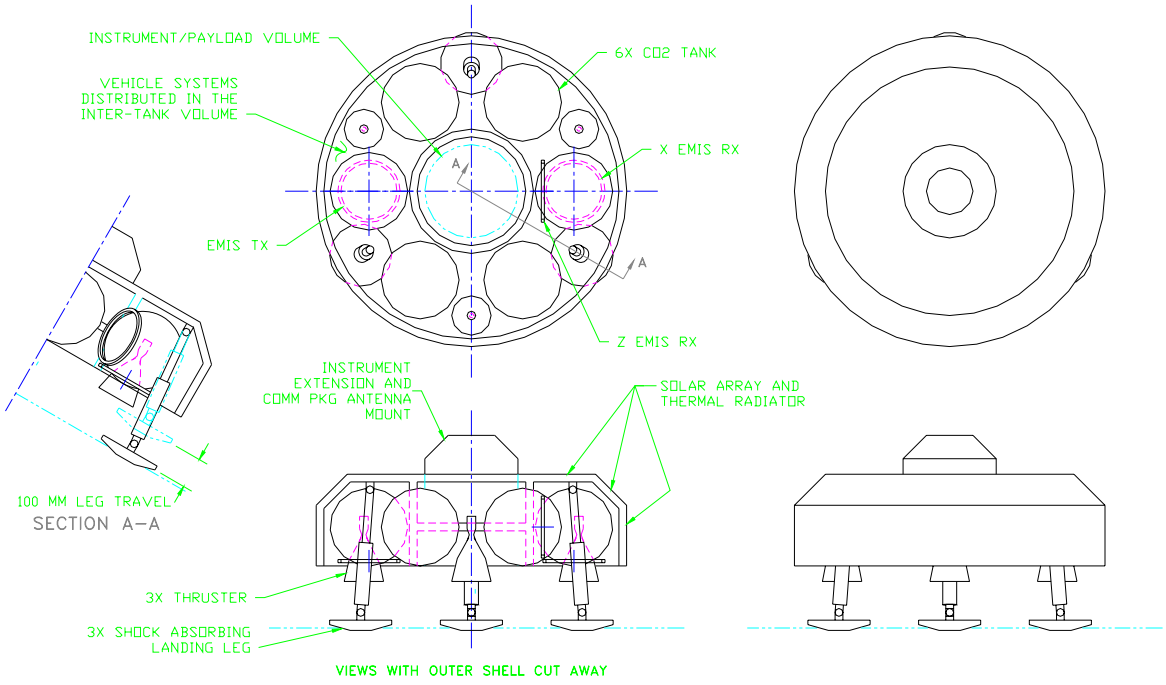

Figure 1, Skimmer

Table 1 presents the mass budget. We are maintaining a contingency mass of 20 kg, or approximately 25%. The contingency mass is not included in the FE model, but has been included in calculations to determine propellant requirements and control parameters.

Table 1, Mass Budget

Subsystem	Mass Budget (kg)	Basis of Estimate
Instrument	14.0	allocation
Payload	2.5	allocation
Structure	29.0	FE model
Camera + electronics	3.0	allocation
Compressor (600 to 37200 Pa)	7.5	FE model + electronics estimate
Drill + Motor	4.0	allocation
Solar Cells	2.5	0.8 m^2 18% efficiency - two 6 hour days
Battery	10.0	estimate for 2370 kJ + 50% contingency
Flight Control System	2.5	allocation
Fuel	5.0	estimate
Subtotal	80	
Contingency	20	25%
Total	100 kg	

The weight estimates were based on the following environmental and operating scenario assumptions:

Temperature range: 173 ^{o}**K** - 273 ^{o}**K** (night minimum, day maximum)
Martian atmosphere: 600 Pa, 95.3% CO_2
Martian gravity: 3.7 m/sec ^{2}

3.0 Mechanical Analysis

3.1 Structural Design & FE model

A system level finite element model has been developed in Nastran (UAI), along with FEMAP pre and postprocessor. The model has been used to determine mass property and to permit normal modes predictions. Eventually, it will also be used to perform loads analysis.

The model development, in conjunction with normal modes results was also used to determine stiffness characteristics of subsystem supports.

The model, shown in Figure 2, consists of 666 grids and 987 elements. The model is a combination of beam and plate elements. The mass of the structure is 75 kg, plus 5 kg of fuel, for fully loaded configuration.

The pitch mass moment of inertia, used in the simulation is for the full fuel tank case and is 13.8 kg-m^2.

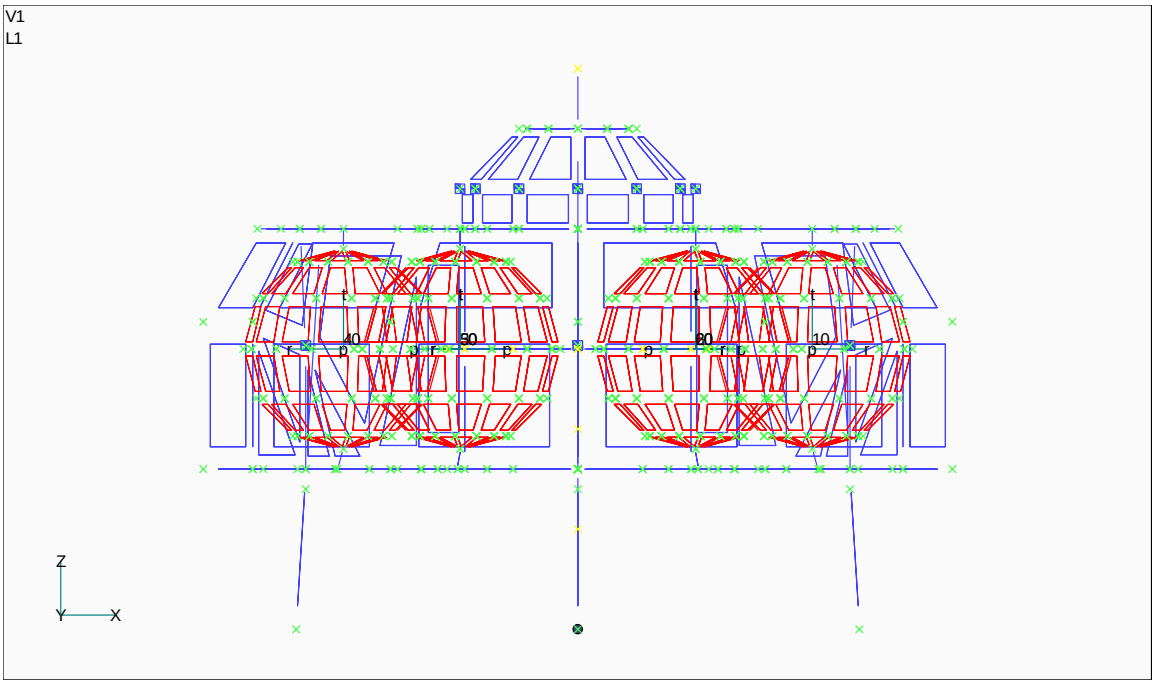

Figure 2. Finite Element Model

Table 2 presents the lowest normal modes of the structure for 4 configurations. The free modes should be high enough in frequency to avoid undesired control system interactions.

Table 2, FE Predicted Normal Modes

	1st mode	2nd mode	3rd mode
grounded, empty fuel tanks	30.9 Hz	30.9 Hz	38.7 Hz
grounded, full fuel tanks	29.56 Hz	29.58 Hz	36.65 Hz
free, empty fuel tanks	49.3 Hz	49.3 Hz	49.4 Hz
free, full fuel tanks	43.2 Hz	45.2 Hz	45.2 Hz

3.2 Propulsion Concept

The propulsion concept is based on in situ resource utilization (ISRU) of the Mars atmosphere and the use of solar energy as the power source. There are other similar concepts: Zubrin et al [2] and Landis and Linne [3] have studied longer range Martian transportation vehicles, based on CO_2 ISRU.

We have an early stage concept for compression of the Martian atmosphere to dry ice/snow. It is based on a smart structure fan, running at a resonance. It is estimated to be capable of generating 5 kg of compressed CO_2 in < 8 hours using 65 watts of power. The compression stage is assumed to take place in cooler, night time conditions and the transportation stage to take place in warmer, daytime conditions.

The compression stage will generate heat. It may be desirable to slow the compression stage, to optimize the thermal balance. The increase from night time temperature, to daytime temperature results in the CO_2 pressure rising to 8 MPa. On exhausting the compressed CO_2, to atmospheric conditions, the equivalent specific impulse is 56 seconds.

For a 100 kg vehicle to hover on Mars requires 370 N of thrust. The 5 kg of compressed CO_2 (specific impulse of 56 seconds) will provide about 7.5 seconds of hover time

4.0 Vehicle Control Approach

There are several possible approaches to the control of this vehicle:

1. Use of a single large thruster on the vehicle's vertical axis; rotation of the whole vehicle by means of separate rotation control devices (thrusters, control moment gyros, etc) to vary the thrust direction;
2. As in (1) but with multiple vertical thrusters located outboard;
3. As in (2) but with differential throttling of the thrusters to effect rotation control instead of using separate rotation control devices;
4. Separate vertical and horizontal thrusters, with the vehicle flying in a level attitude.

Approach (1) would conflict with the desire to leave the vehicle's center free for the drill. Of the others, option (3) appears to be most desirable because it uses the least hardware. One goal of the simulation described here was to examine this viability of this approach. It was found that it does appear to be viable, though the short duration of the flights of this vehicle will require a quite agile control system to make use of it.

5.0 Flight Simulation

5.1 2-Impulse Trajectories

Impulsive maneuvers, i.e., instantaneous changes in velocity in discrete steps, are usually optimal in the sense of requiring minimum total delta-V in trajectory problems. In the case of a vehicle performing a hop over a surface in a gravity field, a trajectory of this sort would consist of: (1) takeoff involving an instantaneous change to an inclined initial velocity; (2) coasting on a parabolic path (ignoring air resistance which is a good approximation here); (3) instantaneous deceleration to zero speed on returning to the ground.

These instantaneous accelerations would require infinite thrust, and so are not achievable in practice. However, the resulting flight can serve as an ideal against which real trajectories can be compared.

For such an impulsive flight, minimum total delta-V is achieved by having the initial velocity after step 1 be inclined at 45 degrees (actually for minimum propellant mass consumption this may not be quite optimum, but for the small propellant masses involved with this vehicle the difference will be small). The launch and landing velocity changes are then each $\sqrt{ad}$ where a is the gravitational acceleration and d the distance to be traveled. Applying the rocket equation at each end of the path, the propellant mass required for such a flight would be

$$m_{prop} = m_{GTO}\left[1 - \exp\left(\frac{-2\sqrt{ad}}{u}\right)\right] \qquad (1)$$

where m_{prop} is the propellant mass required; m_{GTO} is the vehicle gross takeoff mass (empty mass plus propellant); u is the thruster effective exhaust velocity (related to the more common rocket performance

parameter, specific impulse as I_{sp} times Earth's gravitational acceleration). This relation is plotted as the lower curve in Figure 5. That curve gives m_{prop} versus d for the parameters we are considering here (m_{GTO} = 100 kg, u = 549 m/s (corresponding to I_{sp} = 56 seconds), and a = 3.7 m/s^2 for Mars's gravity).

5.2 Numerical Integration for More Realistic Trajectories

For a vehicle making a long hop, the trajectory could be arranged to be close to the 2-impulse ideal by concentrating the propulsion at each end of the path. However, for the vehicle we are considering here the flight is so short that with reasonable thrust and pitch control levels, this 2-impulse, ballistic path approximation is a poor one. Also certain science requirements make specialized flight paths useful. As a result, more elaborate flight plans must be considered. Propellant mass requirements for the vehicle can then be defined or verified on the basis of these flight plans.

To examine these more realistic trajectories, a simulation was written. This is a custom C++ program that simulates the planar motion of the vehicle. In terms of a Cartesian coordinate system, the vehicle moves in the X-Z plane. Three degrees of freedom in total are included in the simulation: horizontal and vertical translation, x and z, and pitch angle, θ, which is rotation about the Y axis. Figure 3 shows snapshots of the vehicle during a simulation along with the simulation's global coordinate system. Translation in Y and rotations about the X and Z directions were not included in order to improve computation speed for the optimization steps described below. In practice the vehicle's nominal trajectory will almost certainly be planar. The extra degrees of freedom will need to be included for control system simulation, but for trajectory planning purposes the 3 dof-s used here are sufficient.

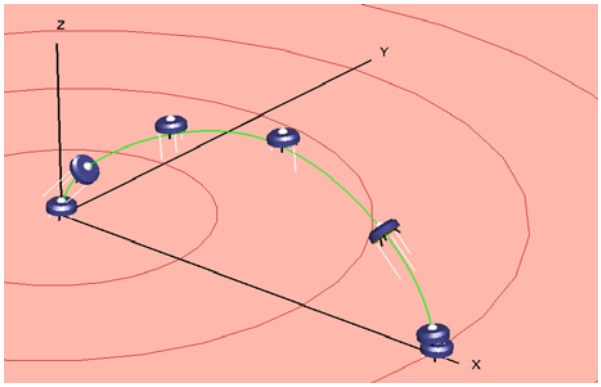

Figure 3, Typical numerical simulation result

Maximum excursion: x~ 15m; z~5m

The simulation s/w allows entry of thrust and pitch moment schedules and simulates the vehicle's flight from takeoff to landing. It uses a standard Runge-Kutta numerical integration approach. Free-flight aerodynamics is included, though not yet ground effect aerodynamics during takeoff and landing.

5.3 Flight Plan Optimization Using the Numerical Integration Simulation

Flight plans (thrust and pitch moment schedules) can be generated by manual adjustment until the desired range is achieved in the simulation with a smooth touchdown. However, this is not particularly easy. Because in the course of design this will need to be done many times with different parameters and flight needs, this was not an efficient option. The ideal approach would be to use optimization software to develop a flight plan that simultaneously meets constraints on the flight path (soft landing plus other, possibly science-related constraints) while minimizing propellant consumption.

This was explored using two classical optimization approaches: Powell's method, and the Davidson-Fletcher-Powell algorithm [4], the latter with derivatives obtained by numerical differencing. Various penalty functions were experimented with to generate an objective function that would satisfy constraints while minimizing propellant consumption. The constraints and propellant consumption were evaluated by simulating the flight for a given set of optimization variables using the numerical integration simulator described above. The optimization variables were taken to be thrust force and pitch moment values at discrete times during the flight, with linear interpolation of these parameters between the discrete times.

A multi-objective genetic algorithm (GA), the SPEA2 method [5] with both standard recombination operators and those of [6], was also tried.

None of these proved particularly effective. There appeared to be numerous local minima in the objective function landscape. Also, a considerable amount of the optimizer's effort appeared to be expended in trying to satisfy the constraints. As a result, the propellant consumption minima found were only marginally better than that for flight plans derived manually (not as good in many cases).

The difficulty here, which was common to the classical and GA optimization, appeared to be related to the flight plan definition and constraint approach which was being taken. The use of arbitrary thrust and pitch moment schedules as optimization variables, combined with a variety of constraints on the flight involving smooth landing, no ground contact, etc, made for a hard problem. To remove some of this difficulty a different model was created that used a more analytic approach to simulation of the flight. This is described in the following section.

5.4 Analytical Flight Path Model

This model does not involve numerical integration of the flight. Rather it consists of the following:

1. the flight path is defined by a B-spline curve [7]
2. this curve interpolates a small set of waypoints which the vehicle is constrained to pass through at pre-defined times
3. derivative constraints on the B-spline curve are applied at both takeoff and landing (the two ends of the curve) to ensure zero translational velocity, zero pitch and zero pitch rate at those points.

With such a model, optimization variables can be the coordinates of the waypoints and the times at which the vehicle passes through them. These are quite intuitive for flight planning purposes involving science goals. In addition, these parameters are relatively free to be varied. The smooth landing constraints are automatically supplied by the model, and other constraints such as no ground contact during the path proved quite easy to insert. This model is described in more detail in the rest of this section. Results from using it to optimize propellant use and to define some science-requirement hops are described in the following section.

For a vehicle of mass m translating in the X-Z plane, the thrust force with magnitude F and components F_x and F_z is related to the acceleration of the center of gravity by

$$F_x = m\ddot{x} \tag{2}$$

$$F_z = m\ddot{z} + a \tag{3}$$

$$F = \sqrt{F_x^2 + F_z^2} \tag{4}$$

Where a is Mars gravity acceleration. This ignores aerodynamic forces and other disturbances, but the numerical integration simulation showed this to be satisfactory.

Because the thrust force is directed along the vehicle's axis for the differential thrust pitch control case being modeled here, there is a further relation connecting the thrust force components and the pitch angle:

$$\theta = \arctan\left(\frac{F_x}{F_z}\right) = \arctan\left(\frac{\ddot{x}}{\ddot{z} + a}\right) \tag{5}$$

where the equality has made use of equations (2) and (3). Differentiating this relation gives the pitch rate

$$\dot{\theta} = \frac{(\ddot{z}+a)\,\dddot{x} - \ddot{x}\,\dddot{z}}{\left(\ddot{x}\right)^2 + \left(\ddot{z}+a\right)^2} \tag{7}$$

and differentiating the pitch rate gives the pitch angular acceleration

$$\ddot{\theta} = \frac{(\ddot{z}+a)\,\ddddot{x} - \ddot{x}\,\ddddot{z}}{\left(\ddot{x}\right)^2 + \left(\ddot{z}+a\right)^2} + 2\,\frac{\ddot{x}(\ddot{z}+a)(\dddot{x})^2 + (\ddot{x})^2\,\dddot{x}\,\dddot{z} + (\ddot{z}+a)\,\dddot{x}\,\dddot{z} + \ddot{x}\ddot{x}(\ddot{z}+a)(\dddot{z})^2}{\left[\left(\ddot{x}\right)^2 + \left(\ddot{z}+a\right)^2\right]^2} \tag{8}$$

The pitch moment is then given by $M = I\,\ddot{\theta}$ where *I* is the pitch moment of inertia.

These equations define the thrust force, pitch angle, pitch rate and pitch moment all in terms of the *x(t)* and *z(t)* relations which specify the vehicle position as a function of time. From the thrust force and the pitch moment, the individual forces required at each thruster can be determined.

Because the vehicle is stationary and level at the start of the flight, and because we want a smooth, level landing, the following constraints apply at both the initial and final points of the path:

1. zero translational velocity, $\dot{x} = \dot{z} = 0$.
2. zero pitch angle. From equation (6), this implies $\ddot{x} = 0$.
3. zero pitch rate. From equation (7), after condition 2 is imposed, this implies $\dddot{x} = 0$.

Imposing these derivative conditions on the functions *x(t)* and *z(t)* at the initial and final points of the path will ensure a smooth takeoff and a smooth landing.

The next step is to decide on forms of the functions *x(t)* and *z(t)* which can be used to describe a wide selection of paths in terms of a relatively small set of variables. B-spline functions [7] have been chosen here. These are piecewise polynomials with smoothness constraints between the pieces. They are usually defined in an intuitive geometric fashion. Because of this, they are commonly used in CAD. They have the advantage of being well documented with standard formulas available for their derivatives, they are numerically robust, and they tend to be "smoothing", i.e., they have less tendency to have large excursions between the defining points than more straightforward polynomial fits. These properties are all advantageous in this application.

Given a set of points which a B-spline must pass through, and the set of derivative constraints which the B-spline must satisfy at the beginning and end of the trajectory, the method of [7], section 9.2.4 can be used to define the B-spline. B-splines are parametric curves, and we have used time directly to parameterize them in our case. Because we have different derivative conditions in the X and Z directions, we use separate B-splines to fit X and Z.

The degree of the B-splines must be chosen, i.e., the polynomial degree of the various pieces that the B-spline consists of. Here we have most commonly used degree 6 for the X direction and 5 for the Z direction. These imply continuous thrust and pitch moment function first derivatives. Lower degrees would allow more sudden changes to these control inputs. However, it was found that the additional

smoothness made for smoother appearing flight paths with no penalty in propellant consumption, at least for the parameters being studied here.

The number of waypoints is flexible. Typically we have found 5 to 7 (including the end points) to be sufficient to describe most paths. Five appears to allow enough freedom for the optimization process described below to find reasonably good solutions. Using up to 12 points made very little difference to the optimum solutions found, again, at least for the parameters being studied here.

This analytical model and the numerical integration one were successfully cross-validated by simulating the flights found by the analytical model (Section 5.4) using the numerical integration one (Section 5.2). This was successful.

In summary, this model allows an analytical functional form to be derived for all parameters of the flight from a set of waypoints, and ensures that the flight has a smooth takeoff and landing. Use of the model is described in the following section.

5.5 Flight Plan Optimization Using the Analytic Flight Path Model

A series of optimum trajectories were generated using this model. Optimization used Powell's method and the optimization variables were the waypoint coordinates and times and the time at the final (landing) point. Each case was for fixed takeoff and landing point locations. The objective function was primarily designed to minimize propellant mass consumption by having its principal term equal to the propellant mass used during the hop. In addition, however, penalty functions were imposed to:

- Limit the maximum thruster force over the flight.
- Eliminate negative thruster forces. These can arise if large pitch moments occur simultaneously with small thrusts for the differential throttling approach being considered.
- Eliminate ground contact. This was deemed to occur if any point between the initial and final locations on the path had zero or negative altitude.
- Eliminate “ground dragging” trajectories. These were deemed to be those with more than 10% of the flight path below a 1 m altitude.

Figure 4 shows some of the resulting minimum propellant flight paths for a maximum thruster force of 500 N. Figure 5 shows the propellant consumption versus flight distance for these paths. This plot also shows the 2-impulse case from equation (1). It can be seen that the restricted thruster force and the need to control pitch attitude implies a noticeable deviation from the 2-impulse, infinite control authority, case. From this data, and allowing small amounts for flight contingency and tank ullage, the requirement of 5 kg of propellant was derived (Table 1) for a 15 m flight.

This study has shown that a 3-thruster, differential throttling propulsion system is possible for this vehicle. Figure 6 shows the pitch angle versus time during the 15 m flight. It can be seen that fairly large and quick changes to the vehicle attitude must occur. This implies an agile control system, and careful pre-planning of the trajectory to avoid any need for terminal maneuvers to steer clear of hazards. This is possible here because the short flight distance allows the destination to be thoroughly characterized visually before the hop begins. However, it is possible that further study will show that this control approach is not optimum. The alternative approach of separate horizontal and vertical thrusters may include complexity and mass penalty. These may need to be weighed against science benefits.

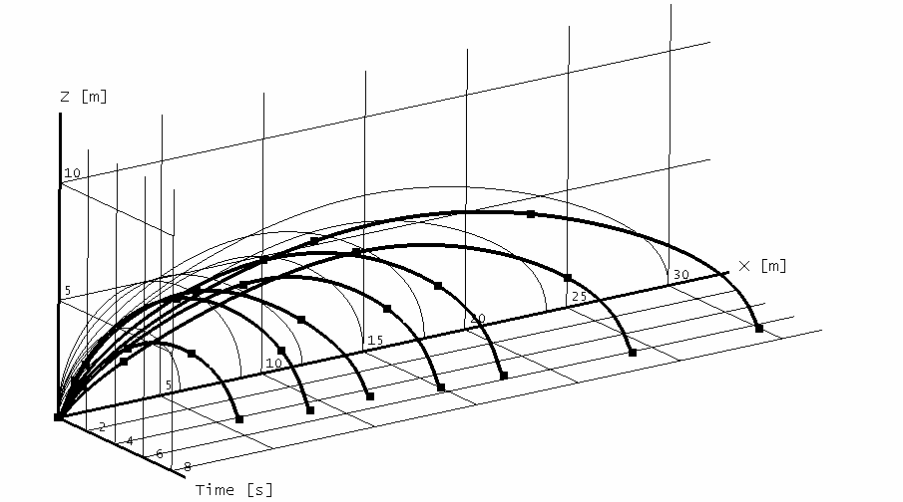

Figure 4 Optimal trajectories, XZ position versus time. Thin line curves show paths in XZ space. Waypoints defining the curves are shown as the small squares.

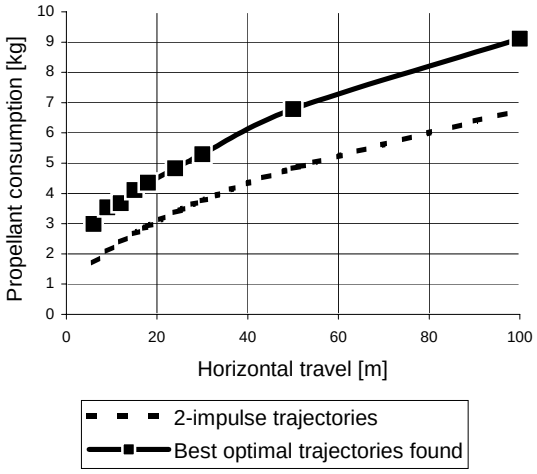

Figure 5 Propellant consumption versus range for trajectories with real system constraints,and for 2-impulse trajectores of eqnation (1)

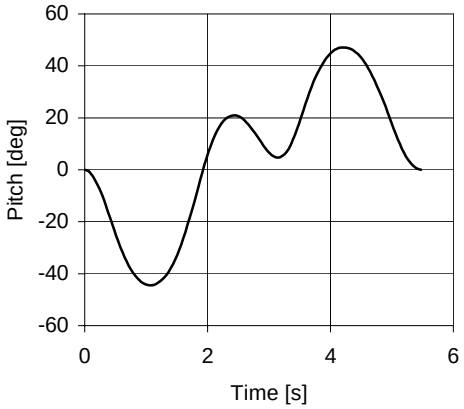

Figure 6 Pitch angle versus time for optimal 15 m hop. Positive is nose up.

Other trajectories may be needed which are not propellant optimal. One type is a vertical hop, used to calibrate the on-board EMIS science sensors. The vehicle is capable of reaching an altitude of 15 m with 5 kg of propellant and the same thruster restrictions as described above. Another type of trajectory is a near constant altitude hovering hop to allow higher fidelity science data acquisition during the hop than is possible with the more parabolic optimal trajectories. Figure 7 shows such a 'hop'. The near constant altitude, 15 m horizontal hop shown would require 5.19 kg of propellant, about 26% more than the optimal 15 m trajectory.

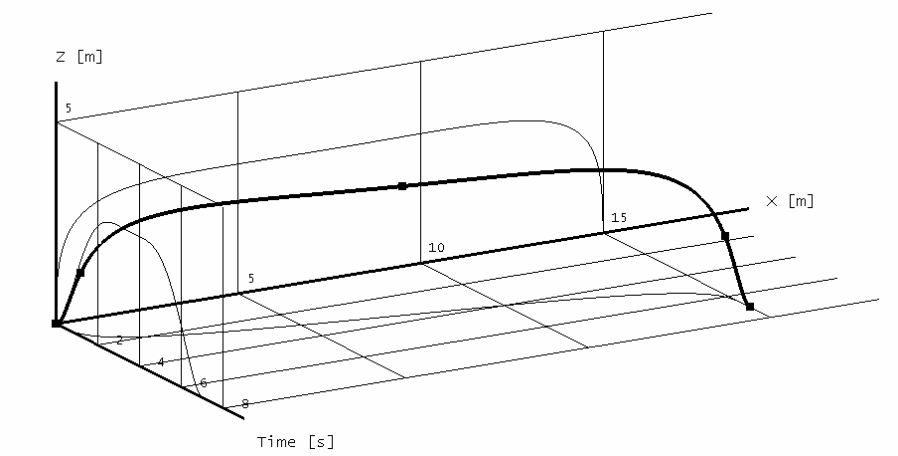

Figure 7 Near constant altitude 15 m hop. Also shown are XZ path and X and Z versus time curves.

6.0 Conclusions

A simulation has been developed which allows some engineering assumptions to be verified and offers initial planning data for the development of scientific instrumentation. The 5 kg of CO_2 propellant needed to achieve transportation and mapping goals has been confirmed as reasonable. The structural parameters (mass properties and structural frequencies) needed to begin the control design of the vehicle have been provided with an initial finite element model. These same properties are also valuable in assessing the environment conditions which occur for various earth launch opportunities.

The use of a simulation as a tool in system design is not novel, but this simulation has been intended to provide a more inclusive design environment. The use of an in-house simulation tool has been chosen, for these initial studies, because it allows for access and control to modify the simulation characteristics – in ways which may not all be apparent. This vehicle is novel, largely because it operates in conditions which remain fairly novel and unexplored to the engineering community.

References

[1] Proposal for a Martian Transportation Vehicle – Concept Study. Good Vibrations Engineering Document: GVE-03-MTV-P01. 2003
[2] Zubrin, Robert et al., 2000. Mars Gashopper. Final Report on NASA Contract No. NAS3-00074, Pioneer Astronautics.
[3] Landis & Linne, 2001. Mars Rocket Vehicle Using In Situ Propellants. Journal of Spacecraft and Rockets (Vol. 38, No. 5);pp730-735
[4] Press, William H., et al. Numerical Recipes in C, Cambridge University Press, 1988.
[5] Zitzler, Eckart, et al. The Strength Pareto Evolutionary Algorithm (SPEA), TIK-Report 103, ETH, Zurich, 2001.
[6] Rasheed, Khaled, et al. A Genetic Algorithm for Continuous Design Space Search, Artificial Intelligence in Engineering, 11(3), 1997.
[7] Piegl, Les A., Tiller, Wayne. The NURBS Book, Springer-Verlag, 1997.